Applied Physics Letters

RESEARCH ARTICLE | JULY 17 2024

Wafer-scale bonded GaN–AlN with high interface thermal conductance

Special Collection: Advances in Thermal Phonon Engineering and Thermal Management

Man Li ; Kaicheng Pan ; Yijun Ge; Kenny Huynh; Mark S. Goorsky ; Timothy S. Fisher ; Yongjie Hu

Appl. Phys. Lett. 125, 032104 (2024)
https://doi.org/10.1063/5.0206263

Articles You May Be Interested In

Experimental determination of critical thickness limitations of (010) β -(Al $_x$Ga$_{1-x}$)$_2$O$_3$ heteroepitaxial films

Appl. Phys. Lett. (November 2023)

(Ultra)wide bandgap semiconductor heterostructures for electronics cooling

Appl. Phys. Rev. (November 2024)

Electronic transport anisotropy of buckling graphene under uniaxial compressive strain: *Ab initio* study

Appl. Phys. Lett. (February 2012)

26 January 2025 21:38:07

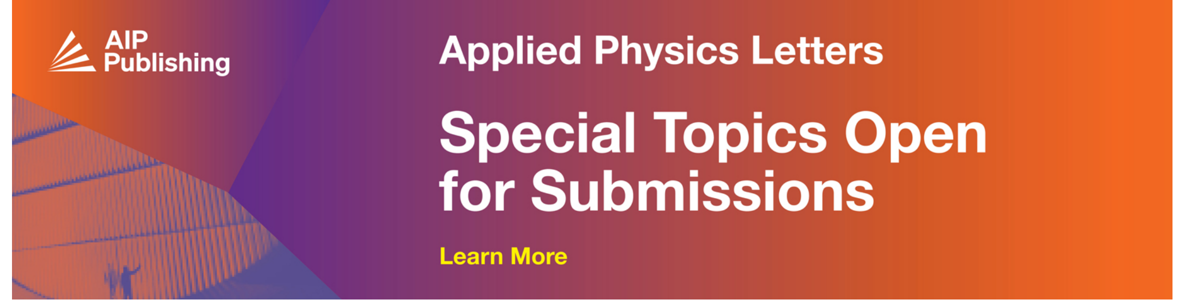

Applied Physics Letters ARTICLE pubs.aip.org/aip/apl

Wafer-scale bonded GaN–AlN with high interface thermal conductance

Cite as: Appl. Phys. Lett. **125**, 032104 (2024); doi: 10.1063/5.0206263
Submitted: 29 February 2024 · Accepted: 19 June 2024 ·
Published Online: 17 July 2024

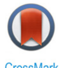

Man Li,[1] Kaicheng Pan,[2] Yijun Ge,[1] Kenny Huynh,[2] Mark S. Goorsky,[2,a)] Timothy S. Fisher,[1,a)] and Yongjie Hu[1,a)]

AFFILIATIONS

[1]Department of Mechanical and Aerospace Engineering, University of California, Los Angeles, Los Angeles, California 90095, USA
[2]Department of Materials Science and Engineering, University of California, Los Angeles, Los Angeles, California 90095, USA

Note: This paper is part of the APL Special Collection on Advances in Thermal Phonon Engineering and Thermal Management.
[a)]**Authors to whom correspondence should be addressed:** goorsky@seas.ucla.edu; tsfisher@ucla.edu; and yhu@seas.ucla.edu

ABSTRACT

Wide and ultrawide bandgap semiconductors, such as GaN, play a crucial role in high-power applications, yet their performance is often constrained by thermal management challenges. In this work, we introduce a high-quality interface between GaN and AlN, prepared through wafer-scale bonding and verified via high-resolution transmission electron microscopy and transport experiments. We experimentally measured the thermal boundary conductance of the GaN–AlN interface, achieving up to 320 MW/m^{2}K at room temperature using an ultrafast optical technique and sensitivity examinations. Non-equilibrium atomistic Green's functions and density functional theory simulations were conducted to model the interface phonon modes and their contributions to thermal transport, demonstrating good agreement with the experimental results from 80 to 300 K. Additionally, we observed a size-dependent effect on the thermal boundary conductance related to the GaN film thickness from 180 to 450 nm, which we attributed to quasi-ballistic thermal transport through molecular dynamics simulations. Our study has demonstrated a scalable processing route for wafer-sized chip packaging and provides fundamental insights to mitigate near-junction thermal resistance. Further exploration of interface engineering could facilitate co-design strategies to advanced thermal management technologies.

Published under an exclusive license by AIP Publishing. https://doi.org/10.1063/5.0206263

26 January 2025 21:38:07

Wide and ultrawide bandgap semiconductor materials play a critical role in emerging technologies from power electronics, optoelectronics, photonics, to quantum devices.[1–3] However, thermal management of high-power devices represents one of the most formidable challenges.[4–10] The demand for heat dissipation in gallium nitride (GaN)-based devices has been escalating as the power density is anticipated to approach nearly 1 MW/cm^2 by 2030 and posed a considerable impact on device performance, stability, and lifetime.[10] In particular, interfacial heat transfer between adjacent materials layers, characterized by its thermal boundary conductance (TBC), has been recognized as a major contribution to the total thermal resistances that restrict heat dissipation.[4] In this study, we performed the experimental measurements of TBC at the interfaces between GaN and aluminum nitride (AlN) in wafer-size bonded samples. The experimental structure was systematically analyzed with measurement sensitivity and atomistic modeling to provide reliable determination of a high interface thermal conductance up to 320 MW/m^{2}K. The interface quality of the bonded GaN–AlN was also examined through transmission electron microscopy imaging and temperature-dependent measurements of TBC using time-domain thermoreflectance (TDTR). We observed a size effect in TBC from the measurements and attributed it to quasi-ballistic thermal transport in the confined GaN layer. The contributions to TBC from spectral-dependent phonon transmission were revealed using atomic Green's function with density functional theory (DFT) and molecular dynamics (MD) simulations. The study provides fundamental insights and future co-design guideline for thermal management of wide and ultrawide bandgap semiconductors.

Fundamentally, TBC of semiconductor interfaces arises from multi-scale contributions including atomistic interface scattering, incomplete microscale contacts, and disorders near the interface, which have been thoroughly discussed in the recent review.[4] For materials grown under optimized conditions, the TBC limit is defined by the breakdown of coherent phonon transport at heterogeneous junctions due to phonon spectral mismatching.[4] The interface between AlN and GaN is especially important as a critical element in forming AlGaN epitaxial layers and is indispensable for 2D electron gas and

Published under an exclusive license by AIP Publishing

high electron mobility transistors (HEMTs). The structural isomorphism between AlN and GaN, along with the matching of their lattices and thermal expansions, allows for the creation of abrupt compositional junctions and the realization of desired functionalities. In the literature, the TBC of GaN and AlN has been of high interest for modeling studies;[11,12] however, experimental measurements have yet to be reported for a pristine GaN–AlN heterostructure, particularly for samples on a wafer scale.

Here, we introduce an optimized direct bonding approach to establish high-quality interfaces between GaN and AlN on a wafer scale. Our bonding process is illustrated in Fig. 1(a). The Ga-face of the GaN wafer was bonded to the N-face of the AlN wafer, using commercially available GaN (2 in., 400 μm thick from Unipress) and AlN wafers (2 in., 400 μm thick from Hexatech). The as-received Ga-face of the GaN substrates exhibited a roughness of less than 1 nm, while the N-face of the AlN substrates had an initial roughness of approximately 3 nm. We first conducted chemical-mechanical polishing to reduce the roughness of the AlN to less than 1 nm, based on our previous work with GaN.[13] Prior to bonding, the wafers were dipped into diluted HF: H_2O solution to remove any surface oxides that existed on the wafer surfaces. After the HF treatment, the wafers were immediately submerged into a $(NH_4)_2S$ solution for surface passivation. Afterward, the samples were rinsed, dried, and pressed under low applied pressure ($\sim$50 kPa). This process was based on our previous wafer bonding works with other III–V materials (GaAs, InP)[13–16] and the parameters described led to a well-bonded interface. As shown in the inset of Fig. 1(b), a significant fraction of the wafer surfaces was bonded, except for a couple of triangular regions associated with growth sector boundaries in the GaN. Subsequent annealing up to 800 °C was performed (GaAs and InP, for example, were annealed at 200°–400° for 1–24 h[14]) to strengthen the bonding and to test the structure for high temperature stability. The similar thermal expansion coefficients and lattice constants between GaN and AlN[17,18] allows for the high-temperature annealing without debonding or cracking. To verify the structural quality, we performed high-resolution transmission electron microscopy (TEM) imaging on the GaN–AlN sample. Figure 1(b) shows the imaging results, revealing the atomically resolved interface. The cross-sectional TEM image displays only a $\sim$1.5 nm interfacial region, which is attributed to the possible structural reconfiguration of the interfaces (noting that this is approximately the sum of the pre-bonded surface roughness layers) after a multi-step annealing process for the sample (at 350 °C for 22 h, 600 °C for 1 h, and 800 °C for 1 h). Other methods using surface activated bonding, plasma treatment, or other interfacial layers (SiN, Ti, etc.) typically results in an amorphous or oxide layer with a thickness of 2 nm or higher,[19–21] while in this work, a thinner and fully crystalline interface is observed. For thermal transport across the bonding interface, usually the foreign interlayer is desired to be thin to avoid possible additional resistance.[22,23] Noteworthy to mention, for this reported processing, our wafer bonding procedure was carried out at room temperature, ambient atmosphere, and at low bonding pressures (compared to typical bonding forces on the MPa scale), signifying the simplicity of the process.

We performed direct measurements of the TBC between the GaN–AlN interfaces using the time-domain thermoreflectance (TDTR) method. TDTR is an established thermal technique for providing reliable characterizations of interface thermal conductance, and we have utilized it for measurements across a wide range of materials,[5–7,24–29] including heterostructures of GaN with high thermal conductivity boron arsenide (BAs) cooling substrates.[5] To enhance the measurement sensitivity for the bonded GaN–AlN samples, we prepared GaN samples with controlled thickness by grinding and polishing the GaN film to less than 500 nm, as illustrated in Fig. 2(a). During TDTR measurements, a thin aluminum film was deposited on the sample to act as a transducer for converting pump laser energy into thermal excitation and as a sensor for temperature detection. The basic operation of TDTR is schematically represented in Fig. 2(b): the incident pump pulse causes an instantaneous temperature rise with a $\sim$75 fs pulse width, inducing a detectable temperature change by the probe beam. The arrival time difference between the pump and probe pulses is controlled with sub-picosecond resolution using a mechanical delay stage. The collected data are then analyzed using a multilayer thermal model to determine TBC and thermal conductivity (κ). More details about the experimental setup and modeling analysis can be found in our previous publications.[26,27]

To ensure measurement accuracy, we conducted calibration experiments and sensitivity analysis. Calibration experiments were carried out on GaN and AlN samples to ascertain the properties of the heterostructure, including those of the AlN and Al-GaN interfaces. We performed TDTR measurements on these wafers, determining the thermal conductivity of AlN to be 329 ± 29 W/mK and the thermal

26 January 2025 21:38:07

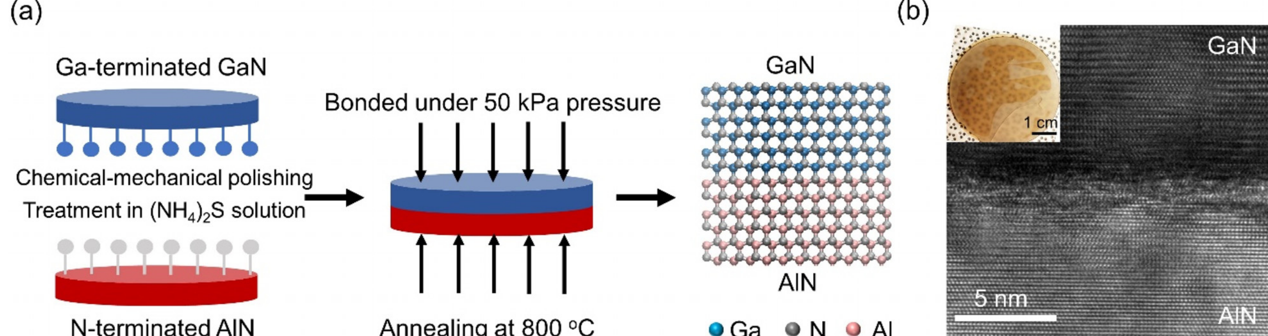

FIG. 1. Fabrication procedure for our wafer-scale bonding process and the characterization of GaN–AlN interfaces. (a) Schematic diagram of the bonding process between GaN and AlN wafers. (b) High-resolution transmission electron microscope (TEM) image of the GaN–AlN interface. Inset, optical image of a wafer-scale sample during bonding.

Published under an exclusive license by AIP Publishing

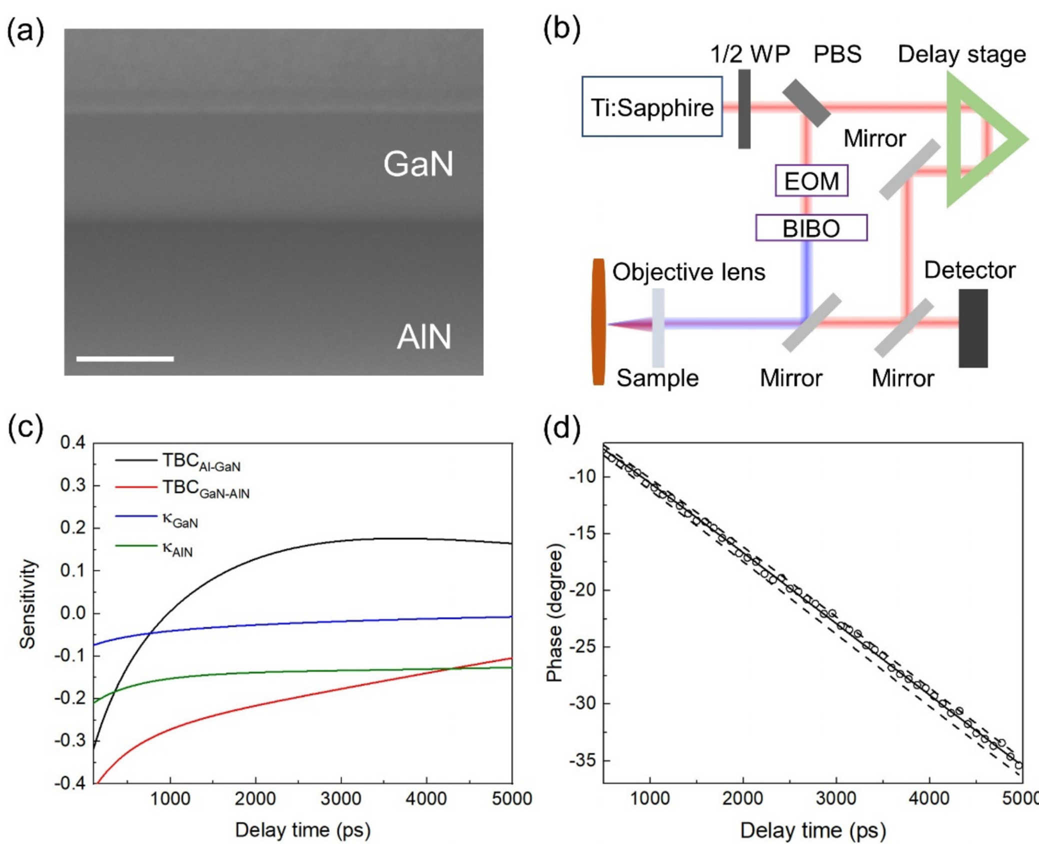

FIG. 2. Thermal transport experiments and measurement sensitivity modeling for GaN–AlN interface structures. (a) A cross-sectional scanning electron microscope image of a GaN–AlN interface sample. Scale bar: 200 nm. (b) A schematic of the time-domain thermoreflectance (TDTR) experimental setup. WP: waveplate; PBS: polarizing beam splitter; EOM: electro-optic modulator; BIBO: bismuth borate. (c) Sensitivity analysis and thermal modeling for the experimental structure of Al–GaN–AlN. The GaN layer is 200 nm thick for the plot. (d) Experimental data from TDTR measurements (circles) are plotted along with the best fit (solid line), compared with ±10% variation in thermal conductance (dashed lines).

boundary conductance (TBC) of Al-GaN to be 87 ± 7 MW/m^{2}K at room temperature. Utilizing the calibrated values, we conducted a modeling analysis to ensure high measurement sensitivity to the thermal conductance of GaN–AlN. The measurement sensitivity is quantified according to the standard definition,[27,30,31] $S_\alpha = \frac{\partial \ln(\theta)}{\partial \ln(\alpha)}$, which represents the change in the measurement signal induced by the variation of an interested parameter. Sensitivity analysis was performed for various parameters, such as TBC$_{\text{Al-GaN}}$, κ_{GaN}, TBC$_{\text{GaN-AlN}}$, and κ_{AlN}, and GaN thicknesses ranging from 150 to 500 nm. The sample structures and thicknesses are thus optimized to achieve high measurement sensitivity to TBC$_{\text{GaN-AlN}}$, as exemplified in Fig. 2(c). Consequently, we prepared the heterostructure samples with GaN thickness within this range. Figure 2(d) presents example TDTR measurement data alongside the model fit and a ±10% variation of thermal conductance, offering a reliable determination of thermal conductance.

The thermal conductance of GaN–AlN interfaces, measured with temperature dependence, is presented in Fig. 3(a). The TBC value increases from 77 MW/m^{2}K at 80 K to 320 MW/m^{2}K at 300 K, indicating typical crystalline behavior.[4,5,26,32,33] By comparison, the measured TBC of GaN–AlN in this study is among the highest compared to other GaN–AlN–X (X: SiC, Si, or diamond) interfaces. It should be noted that in the literature, AlN is usually used as a buffer layer deposited between GaN and other materials with the aim of enhancing TBC. For instance, at room temperature, TBC values reported in the literature typically fall below 50 W/m^{2}K for GaN–diamond interfaces due to intrinsic phonon mismatch and defects[34,35] and increases to 60–100 W/m^{2}K for GaN–AlN–diamond;[36,37] for GaN–silicon or GaN–SiC interfaces, using an AlN buffer layer could improve TBC up to 200 MW/m^{2}K due to better phonon spectral matching.[32,38–40] Here, the measured high TBC of up to 320 MW/m^{2}K for GaN–AlN indicates that the reported interfaces involving an AlN buffer layer may be limited by defects-induced thermal resistance rather than intrinsic resistance. Meanwhile, we also note that the intrinsic TBC of heterostructure interfaces is fundamentally limited by phonon spectral matching.[4,5]

To model the TBC of the GaN–AlN interface, we applied the non-equilibrium Green's function method, utilizing accurate force constants derived from density functional theory (DFT) calculations. Figure 3(b) presents a schematic of the interface structure used in our modeling, where AlN was strained to match the lattice constants of

Published under an exclusive license by AIP Publishing
26 January 2025 21:38:07

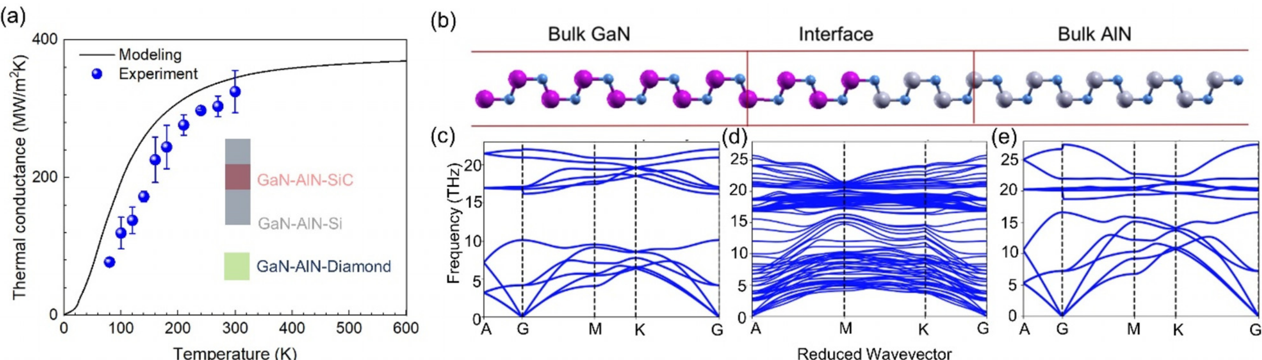

FIG. 3. Experimental measurement and atomistic Green's functions modeling results for thermal boundary conductance (TBC) of the GaN–AlN interface. (a) Temperature-dependent TBC from measurements and calculations with atomic Green's functions. Also plotted are literature reports on GaN interfaces with an AlN buffer layer. (b) A schematic of the GaN–AlN atomic interfaces in density functional theory calculations, where AlN is strained to match the lattice constants of GaN and form bonds between Al and N atoms at the interface. (c)–(e) Calculated phonon dispersions for GaN, the supercell of GaN–AlN interface and AlN.

GaN, forming an abrupt interface created by bonding Al atoms with N atoms. The DFT approach used a plane wave basis set as implemented in the Quantum Espresso suite of codes as in prior work,[41] using Rappe–Rabe–Kaxiras–Joannopoulos ultrasoft pseudopotentials. The generalized gradient approximation with the Perdew–Burke–Ernzerhof functional form approximates the exchange correlation energy. Three sets of first-principles calculations were performed for the results reported here, involving calculations on bulk GaN, bulk AlN, and a GaN–AlN interface supercell. Structural relaxation minimized Hellmann–Feynman forces below 10^{-3} eV/Å. Density functional perturbation theory was used to extract phonon dynamics, with dynamical matrices extracted from $4 \times 4 \times 3$ q-point grids in the bulk materials and a $4 \times 4 \times 1$ q-point grid for the interface supercell. A Fourier transform of the dynamical matrices allows the extraction of interatomic force constants used in Green's function transport calculations and phonon dispersion curves for the three sets of interest, as depicted in Figs. 3(c)–3(e). The good overlap between phonon dispersions of GaN and AlN, together with the broaden phonon channels by interface modes, leads to inherent high TBC. By applying a 10 K temperature difference across the two bulk contacts and solving the non-equilibrium Green's function, we computed Buttiker probe temperatures.[42] The TBC was calculated from the heat flux across the interface and the temperature drop at the interface. The calculated TBC is $\sim$340 MW/m^{2}K when only elastic scattering is considered, close to our measurement result. The consistence between experimental and modeling results regarding the temperature dependence also implies the high quality of the GaN–AlN interface. By contrast, strong phonon-defect scatterings are typically insensitive to temperature variations and can significantly reduce the TBC.[4,43–45]

In addition, we observed a substantial size effect on the TBC by examining samples with varied GaN thicknesses, ranging from 180 to 450 nm. As shown in Fig. 4(a), the experimentally measured TBC increases from $\sim$190 MW/m^{2}K to reach around 320 MW/m^{2}K as the GaN thickness increases from 180 to 450 nm. To understand the size effects on TBC, we performed molecular dynamics (MD) simulations with varied sizes of the simulation domains. We employed nonequilibrium MD simulations, utilizing the methodology detailed in our previous publications.[5,6,26] The interfaces were created by joining two slabs of GaN and AlN, each with a cross-sectional area of 5×5 nm^2 and periodic boundary condition. The Stillinger–Weber potential was used for both materials.[46,47] Periodic boundary conditions were applied on all sides. Initially, the systems were equilibrated under isothermal–isobaric ensemble conditions (300 K and 0 Pa) for 5 ns, followed by a 1 ns relaxation period under canonical ensemble conditions at 300 K. Subsequently, a microcanonical ensemble was maintained for 1 ns. The two ends of the system were frozen and fixed, with their adjacent layers functioning as the heat source and sink, with a constant heat flux introduced across the interface. The temperature drop ΔT at the interface was then sampled after reaching a steady state and used to calculate TBC according to $G = Q/\Delta T$, where Q represents the heat flux per area.

The size effects of TBC are evaluated from the comparison between the experimental and MD simulation results in Fig. 4(a), showing a consistent increase in TBC as the GaN thickness increases. To examine phonon spectral contributions, we calculated the spectral thermal conductance by applying a Fourier transform to the autocorrelation function of the heat current at the interface.[48] As presented in Fig. 4(b), the TBC was decomposed into contributions from a spectrum of phonon modes. From the figure, the interface thermal transport and TBC are predominantly influenced by the phonons with frequencies below 10 THz, which also exhibit significant size dependence. By comparison, higher-frequency phonons (above 10 THz) contribute less to the overall TBC and show negligible size effects. This MD result indicates that the reduction in thermal conductance primarily originates from the suppression of lower-frequency phonons, which have longer mean free paths, and their quasi-ballistic thermal transport.[24,28,29] The thickness confinement of the GaN layer suppresses the availability of the phonon modes near the interface. We note that this conclusion is consistent with the modeling results by Liang *et al.*[49] and Wang *et al.*[50]

In summary, we have developed a wafer-scale bonding process and reported the experimental measurement of GaN–AlN interfaces. The interface thermal boundary conductance measured from the experiment reaches up to 320 MW/m^{2}K. The exhibited strong temperature dependence is attributed to weak scattering by defects in crystals and better approaching the intrinsic limit. The atomic Green's function method, utilizing force constants derived from density functional theory, was adopted to account for the phonon spectra and

26 January 2025 21:38:07

Published under an exclusive license by AIP Publishing

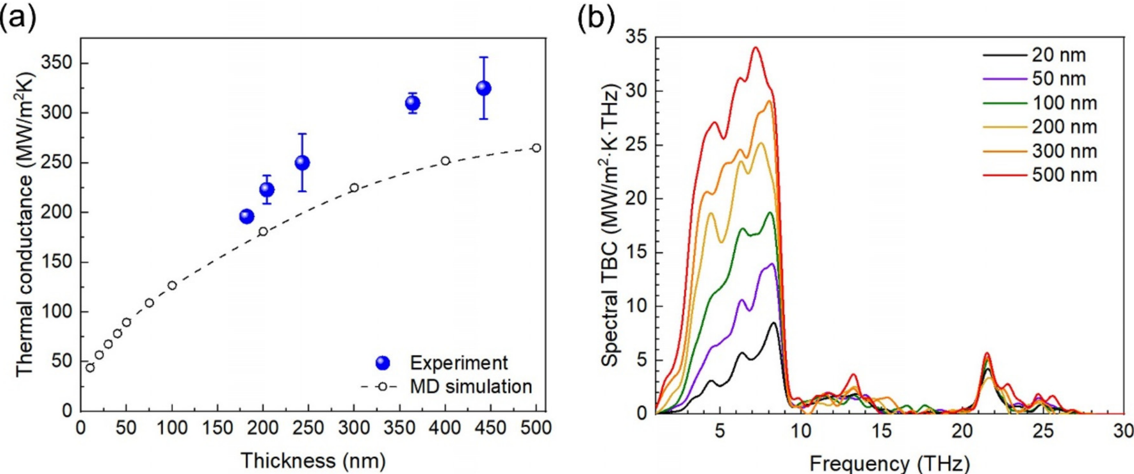

FIG. 4. Size effect on thermal boundary conductance (TBC) from experiments and molecular dynamics. (a) Measurement results of TBC dependent on GaN thickness, plotted alongside molecular dynamics simulation results. (b) Spectral thermal boundary conductance of GaN–AlN interfaces with varied thicknesses of the GaN layers.

calculate the TBC, showing consistency with the experimental results. Additionally, size effects on TBC, dependent on GaN thickness, were experimentally observed and analyzed through molecular dynamics simulations. The size-dependent TBC is attributed to quasi-ballistic thermal transport and the suppression of phonon scattering from long mean free path modes due to thickness confinement. This study has developed a scalable route for manufacturing GaN heterostructures with high TBC interfaces. Further exploration of this bonding approach with materials of ultrahigh thermal conductivity, such as boron arsenide (BAs),[5,24,51] could overcome current thermal budget limitations and significantly improve the heat dissipation and device performance of wide and ultrawide bandgap semiconductors. The combined approach of experimental measurements and modeling analysis, along with electrical studies, could enable advanced thermal management technologies based on electrical–thermal–mechanical co-design strategies.[52–54]

The authors appreciate funding support from the DARPA-SRC JUMP center administered by UC Santa Barbara under task 2778.055.

AUTHOR DECLARATIONS

Conflict of Interest

The authors have no conflicts to disclose.

Author Contributions

Man Li, Kaicheng Pan, and Yijun Ge contributed equally to this work.

Man Li: Conceptualization (equal); Data curation (lead); Formal analysis (lead); Investigation (equal); Methodology (equal); Validation (lead); Visualization (lead); Writing – original draft (lead); Writing – review & editing (equal). **Kaicheng Pan:** Data curation (equal); Formal analysis (equal); Methodology (equal); Validation (equal); Visualization (equal); Writing – review & editing (equal). **Yijun Ge:** Data curation (equal); Formal analysis (equal); Investigation (equal). **Kenny Huynh:** Data curation (equal); Investigation (equal); Methodology (equal). **Mark S. Goorsky:** Conceptualization (equal); Funding acquisition (equal); Investigation (equal); Methodology (equal); Project administration (equal); Resources (equal); Supervision (equal); Writing – review & editing (equal). **Timothy S. Fisher:** Conceptualization (equal); Funding acquisition (equal); Investigation (equal); Project administration (equal); Resources (equal); Supervision (equal); Writing – review & editing (equal). **Yongjie Hu:** Conceptualization (equal); Funding acquisition (equal); Investigation (equal); Project administration (equal); Resources (equal); Supervision (equal); Writing – original draft (equal); Writing – review & editing (equal).

DATA AVAILABILITY

The data that support the findings of this study are available within the article.

REFERENCES

[1]S. Nakamura, "The roles of structural imperfections in InGaN-based blue light-emitting diodes and laser diodes," Science **281**(5379), 956–961 (1998).
[2]U. K. Mishra, L. Shen, T. E. Kazior, and Y.-F. Wu, "GaN-based RF power devices and amplifiers," Proc. IEEE **96**(2), 287–305 (2008).
[3]M. J. Tadjer, "Toward gallium oxide power electronics," Science **378**(6621), 724–725 (2022).
[4]Y. Cui, M. Li, and Y. Hu, "Emerging interface materials for electronics thermal management: Experiments, modeling, and new opportunities," J. Mater. Chem. C **8**, 10568 (2020).
[5]J. S. Kang, M. Li, H. Wu, H. Nguyen, T. Aoki, and Y. Hu, "Integration of boron arsenide cooling substrates into gallium nitride devices," Nat. Electron. **4**(6), 416–423 (2021).
[6]M. Li, H. Wu, E. M. Avery, Z. Qin, D. P. Goronzy, H. D. Nguyen, T. Liu, P. S. Weiss, and Y. Hu, "Electrically gated molecular thermal switch," Science **382**(6670), 585–589 (2023).
[7]S. Li, Z. Qin, H. Wu, M. Li, M. Kunz, A. Alatas, A. Kavner, and Y. Hu, "Anomalous thermal transport under high pressure in boron arsenide," Nature **612**(7940), 459–464 (2022).

26 January 2025 21:38:07

Published under an exclusive license by AIP Publishing

[8]P. Ball, "Computer engineering: Feeling the heat," Nature **492**(7428), 174 (2012).
[9]J. Y. Tsao, S. Chowdhury, M. A. Hollis, D. Jena, N. M. Johnson, K. A. Jones, R. J. Kaplar, S. Rajan, C. G. Van de Walle, E. Bellotti, C. L. Chua, R. Collazo, M. E. Coltrin, J. A. Cooper, K. R. Evans, S. Graham, T. A. Grotjohn, E. R. Heller, M. Higashiwaki, M. S. Islam, P. W. Juodawlkis, M. A. Khan, A. D. Koehler, J. H. Leach, U. K. Mishra, R. J. Nemanich, R. C. N. Pilawa-Podgurski, J. B. Shealy, Z. Sitar, M. J. Tadjer, A. F. Witulski, M. Wraback, and J. A. Simmons, "Ultrawide-bandgap semiconductors: Research opportunities and challenges," Adv. Electron. Mater. **4**(1), 1600501 (2018).
[10]DARPA Microsystems Technology Office, "Technologies for heat removal in electronics at the device scale (THREADS)," Report No. HR001123S0013 (DARPA Microsystems Technology Office, 2022), https://sam.gov/opp/4f04a2bcda114333a426c4d57ffa4081/view.
[11]W. Bao, Z. Wang, and D. Tang, "Phonon transport across GaN/AlN interface: Interfacial phonon modes and phonon local non-equilibrium analysis," Int. J. Heat Mass Transfer **183**, 122090 (2022).
[12]C. A. Polanco and L. Lindsay, "Phonon thermal conductance across GaN-AlN interfaces from first principles," Phys. Rev. B **99**(7), 075202 (2019).
[13]S. Hayashi, T. Koga, and M. S. Goorsky, "Chemical mechanical polishing of GaN," J. Electrochem. Soc. **155**(2), H113 (2008).
[14]M. Jackson, B. L. Jackson, and M. S. Goorsky, "Investigation of sulfur passivation treatments for direct wafer bonding of III-V materials," ECS Trans. **33**(4), 375 (2010).
[15]M. J. Jackson, B. L. Jackson, and M. S. Goorsky, "Reduction of the potential energy barrier and resistance at wafer-bonded n-GaAs/n-GaAs interfaces by sulfur passivation," J. Appl. Phys. **110**(10), 104903 (2011).
[16]K. Yeung, J. Mc Kay, C. Roberts, and M. S. Goorsky, "Electrical conductivity of direct wafer-bonded GaAs/GaAs structures for wafer-bonded tandem solar cells," ECS Trans. **50**(7), 99 (2013).
[17]C. Roder, S. Einfeldt, S. Figge, and D. Hommel, "Temperature dependence of the thermal expansion of GaN," Phys. Rev. B **72**(8), 085218 (2005).
[18]S. Figge, H. Kröncke, D. Hommel, and B. M. Epelbaum, "Temperature dependence of the thermal expansion of AlN," Appl. Phys. Lett. **94**(10), 101915 (2009).
[19]V. Dragoi, N. Razek, E. Guiot, R. Caulmilone, M. Liao, Y. S. Wang, M. S. Goorsky, L. Yates, and S. Graham, "Direct wafer bonding of GaN for power devices applications," ECS Trans. **86**(5), 23 (2018).
[20]F. Mu, Y. Morino, K. Jerchel, M. Fujino, and T. Suga, "GaN-Si direct wafer bonding at room temperature for thin GaN device transfer after epitaxial lift off," Appl. Surf. Sci. **416**, 1007–1012 (2017).
[21]M. Liao, C. Li, C. Flötgen, and M. S. Goorsky, "Characterization of wafer-bonded oxide-free silicon with surfaces treated with an ion-bombardment procedure," ECS Trans. **86**(5), 55 (2018).
[22]S. Wang, D. Xu, R. Gurunathan, G. J. Snyder, and Q. Hao, "Thermal studies of individual Si/Ge heterojunctions—The influence of the alloy layer on the heterojunction," J. Materiomics **6**(2), 248–255 (2020).
[23]Z. Cheng, F. Mu, L. Yates, T. Suga, and S. Graham, "Interfacial thermal conductance across room-temperature-bonded GaN/diamond interfaces for GaN-on-diamond devices," ACS Appl. Mater. Interfaces **12**(7), 8376–8384 (2020).
[24]J. S. Kang, M. Li, H. Wu, H. Nguyen, and Y. Hu, "Experimental observation of high thermal conductivity in boron arsenide," Science **361**(6402), 575–578 (2018).
[25]J. S. Kang, M. Ke, and Y. Hu, "Ionic Intercalation in two-dimensional van der Waals materials: In situ characterization and electrochemical control of the anisotropic thermal conductivity of black phosphorus," Nano Lett. **17**(3), 1431–1438 (2017).
[26]M. Li, J. S. Kang, H. D. Nguyen, H. Wu, T. Aoki, and Y. Hu, "Anisotropic thermal boundary resistance across 2D black phosphorus: Experiment and atomistic modeling of interfacial energy transport," Adv. Mater. **31**(33), 1901021 (2019).
[27]M. Li, J. S. Kang, and Y. Hu, "Anisotropic thermal conductivity measurement using a new asymmetric-beam time-domain thermoreflectance (AB-TDTR) method," Rev. Sci. Instrum. **89**(8), 084901 (2018).
[28]Y. Hu, L. Zeng, A. J. Minnich, M. S. Dresselhaus, and G. Chen, "Spectral mapping of thermal conductivity through nanoscale ballistic transport," Nat. Nanotechnol. **10**(8), 701–706 (2015).
[29]J. S. Kang, H. Wu, and Y. Hu, "Thermal properties and phonon spectral characterization of synthetic boron phosphide for high thermal conductivity applications," Nano Lett. **17**(12), 7507–7514 (2017).
[30]B. C. Gundrum, D. G. Cahill, and R. S. Averback, "Thermal conductance of metal-metal interfaces," Phys. Rev. B **72**(24), 245426 (2005).
[31]A. J. Schmidt, X. Chen, and G. Chen, "Pulse accumulation, radial heat conduction, and anisotropic thermal conductivity in pump-probe transient thermoreflectance," Rev. Sci. Instrum. **79**(11), 114902 (2008).
[32]T. Feng, H. Zhou, Z. Cheng, L. S. Larkin, and M. R. Neupane, "A critical review of thermal boundary conductance across wide and ultrawide bandgap semiconductor interfaces," ACS Appl. Mater. Interfaces **15**(25), 29655–29673 (2023).
[33]J. T. Gaskins, G. Kotsonis, A. Giri, S. Ju, A. Rohskopf, Y. Wang, T. Bai, E. Sachet, C. T. Shelton, and Z. Liu, "Thermal boundary conductance across heteroepitaxial ZnO/GaN interfaces: Assessment of the phonon gas model," Nano Lett. **18**(12), 7469–7477 (2018).
[34]J. W. Pomeroy, M. Bernardoni, D. C. Dumka, D. M. Fanning, and M. Kuball, "Low thermal resistance GaN-on-diamond transistors characterized by three-dimensional Raman thermography mapping," Appl. Phys. Lett. **104**(8), 083513 (2014).
[35]J. Cho, D. Francis, D. H. Altman, M. Asheghi, and K. E. Goodson, "Phonon conduction in GaN-diamond composite substrates," J. Appl. Phys. **121**(5), 055105 (2017).
[36]L. Yates, J. Anderson, X. Gu, C. Lee, T. Bai, M. Mecklenburg, T. Aoki, M. S. Goorsky, M. Kuball, and E. L. Piner, "Low thermal boundary resistance interfaces for GaN-on-diamond devices," ACS Appl. Mater. Interfaces **10**, 24302–24309 (2018).
[37]Y. Zhou, J. Anaya, J. Pomeroy, H. Sun, X. Gu, A. Xie, E. Beam, M. Becker, T. A. Grotjohn, C. Lee, and M. Kuball, "Barrier-layer optimization for enhanced GaN-on-diamond device cooling," ACS Appl. Mater. Interfaces **9**(39), 34416–34422 (2017).
[38]F. Mu, Z. Cheng, J. Shi, S. Shin, B. Xu, J. Shiomi, S. Graham, and T. Suga, "High thermal boundary conductance across bonded heterogeneous GaN–SiC interfaces," ACS Appl. Mater. Interfaces **11**(36), 33428–33434 (2019).
[39]J. Cho, E. Bozorg-Grayeli, D. H. Altman, M. Asheghi, and K. E. Goodson, "Low thermal resistances at GaN–SiC interfaces for HEMT technology," IEEE Electron Device Lett. **33**(3), 378–380 (2012).
[40]G. Yang and B. Cao, "Three-sensor 3ω-2ω method for the simultaneous measurement of thermal conductivity and thermal boundary resistance in film-on-substrate heterostructures," J. Appl. Phys. **133**(4), 045104 (2023).
[41]S. Sadasivam, N. Ye, J. P. Feser, J. Charles, K. Miao, T. Kubis, and T. S. Fisher, "Thermal transport across metal silicide-silicon interfaces: First-principles calculations and Green's function transport simulations," Phys. Rev. B **95**(8), 085310 (2017).
[42]S. Sadasivam, U. V. Waghmare, and T. S. Fisher, "Phonon-eigenspectrum-based formulation of the atomistic Green's function method," Phys. Rev. B **96**, 174302 (2017).
[43]B. Sun, G. Haunschild, C. Polanco, J. Ju, L. Lindsay, G. Koblmüller, and Y. K. Koh, "Dislocation-induced thermal transport anisotropy in single-crystal group-III nitride films," Nat. Mater. **18**(2), 136–140 (2019).
[44]H. Li, R. Hanus, C. A. Polanco, A. Zeidler, G. Koblmüller, Y. K. Koh, and L. Lindsay, "GaN thermal transport limited by the interplay of dislocations and size effects," Phys. Rev. B **102**(1), 14313 (2020).
[45]Q. Zheng, C. Li, A. Rai, J. H. Leach, D. A. Broido, and D. G. Cahill, "Thermal conductivity of GaN, GaN 71, and SiC from 150 K to 850 K," Phys. Rev. Mater. **3**(1), 014601 (2019).
[46]P. Vashishta, R. K. Kalia, A. Nakano, J. P. Rino, C. for, and A. C. Simulations, "Interaction potential for aluminum nitride: A molecular dynamics study of mechanical and thermal properties of crystalline and amorphous aluminum nitride," J. Appl. Phys. **109**(3), 033514 (2011).
[47]A. Béré and A. Serra, "On the atomic structures, mobility and interactions of extended defects in GaN: Dislocations, tilt and twin boundaries," Philos. Mag. **86**(15), 2159–2192 (2006).
[48]K. Sääskilahti, J. Oksanen, J. Tulkki, and S. Volz, "Role of anharmonic phonon scattering in the spectrally decomposed thermal conductance at planar interfaces," Phys. Rev. B **90**, 134312 (2014).

26 January 2025 21:38:07

Published under an exclusive license by AIP Publishing

[49]Z. Liang, K. Sasikumar, and P. Keblinski, "Thermal transport across a substrate–thin-film interface: Effects of film thickness and surface roughness," Phys. Rev. Lett. **113**(6), 065901 (2014).
[50]Q. Wang, X. Wang, X. Liu, and J. Zhang, "Interfacial engineering for the enhancement of interfacial thermal conductance in GaN/AlN heterostructure," J. Appl. Phys. **129**(23), 235102 (2021).
[51]J. S. Kang, M. Li, H. Wu, H. Nguyen, and Y. Hu, "Basic physical properties of cubic boron arsenide," Appl. Phys. Lett. **115**(12), 122103 (2019).
[52]M. Li, L. Dai, and Y. Hu, "Machine learning for harnessing thermal energy: From materials discovery to system optimization," ACS Energy Lett. **7**(10), 3204–3226 (2022).
[53]Z. Qin, M. Li, J. Flohn, and Y. Hu, "Thermal management materials for energy-efficient and sustainable future buildings," Chem. Commun. **57**(92), 12236–12253 (2021).
[54]S. Choi, S. Graham, S. Chowdhury, E. R. Heller, M. J. Tadjer, G. Moreno, and S. Narumanchi, "A perspective on the electro-thermal co-design of ultra-wide bandgap lateral devices," Appl. Phys. Lett. **119**(17), 170501 (2021).

26 January 2025 21:38:07

Published under an exclusive license by AIP Publishing